NASA Technical Memorandum 83364

Friction, Wear, Transfer and Wear Surface Morphology of Ultra-High-Molecular-Weight Polyethylene

Robert L. Fusaro
Lewis Research Center
Cleveland, Ohio

Prepared for the
Joint Lubrication Conference
cosponsored by the American Society of Lubrication Engineers
and the American Society of Mechanical Engineers
Hartford, Connecticut, October 18–20, 1983

NASA

FRICTION, WEAR, TRANSFER AND WEAR SURFACE MORPHOLOGY OF ULTRA-HIGH-MOLECULAR-WEIGHT POLYETHYLENE

by Robert L. Fusaro

National Aeronautics and Space Administration

Lewis Research Center

Cleveland, Ohio 44135

ABSTRACT

Tribological studies at 25° C in a 50-percent-relative-humidity air atmosphere were conducted using hemispherically tipped 400C HT (high temperature) stainless steel pins sliding against ultra-high-molecular-weight polyethylene (UHMWPE) disks. The results indicate that sliding speed, sliding distance, contact stress and specimen geometry can markedly affect friction, UHMWPE wear, UHMWPE transfer and the type of wear mechanisms that occur. Adhesion appears to be the predominant wear mechanism; but after long sliding distances at slow speeds, heavy ridges of transfer result which can induce fatigue-like wear on the UHMWPE disk wear track. In one instance, abrasive wear to the metallic pin was observed. This was caused by a hard particle embedded in the UHMWPE disk wear track. The origin of this particle was uncertain.

E-1629

INTRODUCTION

Polymers and polymer-based composities are increasingly being used for tribological applications. For example, in the aerospace industry they are used in control bearings and in foil bearings (Refs. 1 to 5). One particular polymer that has demonstrated exceptional friction and wear properties is ultra-high-molecular-weight polyethylene (UHMWPE). UHMWPE is currently being used with great success for the replacement of degenerative human joints, such as the hip, knee, and shoulder joints (Refs. 6 and 8).

For ambient-temperature applications, such as the above, UHMWPE performs exceptionally well; however, because differential scanning calorimetry shows it begins to melt at 101° C (Ref. 9), it is not suitable for high-temperature applications. It is important for the development of new polymers and polymer-based composites that will function at higher temperatures, speeds, and loads to better understand how polymers such as UHMWPE lubricate and wear.

This study was conducted to investigate the effect of different sliding speeds on the friction coefficient and wear rates and to determine the wear mechanisms of UHMWPE disks sliding against AISI 440C HT (high temperature) stainless-steel hemispherically tipped pins. Transfer films and UHMWPE wear track surface morphology were studied in an effort to deduce lubricating and wear mechanisms. The effect of varying contact stresses on the wear rate and friction coefficient was also investigated. The results were compared to the results of other researchers (Refs. 8 and 9) who used different test configurations.

MATERIALS

Pin specimens were made of AISI 440C HT stainless steel with a hardness of Rockwell C-58 and a surface finish of 0.09±0.02 μm R_a (arithmetic mean). The disks were made of ultra-high-molecular-weight polyethylene (UHMWPE). They were machined from a block of surgical-grade polymer (RCH 1000). The UHMWPE had a density of 0.937 kg/m^3, a soluble weight-average molecular weight of 2,588,000, and a diamond pyramid hardness of 4.9±0.7 kg/mm^3 (Ref. 9).

APPARATUS

A pin-on-disk tribometer was used to study the tribological properties of 0.476-cm-radius, hemispherically tipped AISI 440C HT stainless-steel pins sliding against 6.3-cm-diameter UHMWPE disks (Fig. 1). The pins were loaded with a 9.8-N deadweight against the flat UHMWPE disk at diameters of 4.0 to

6.0 cm; thus constant speeds of 0.003 to 1.7 m/s were maintained at the rotational speeds of 1-, 10-, 100-, and 800-rpm. The friction specimens were enclosed in a chamber so that atmosphere could be controlled. To obtain an atmosphere of 10 000 ppm H_2O (approx. 50 percent relative humidity at 25° C), dry air was mixed with air bubbled through water.

PROCEDURE

Surface Cleaning

The metal pins were washed with pure ethyl alcohol and then scrubbed with a water paste of levigated alumina. They were rinsed in distilled water and dried with compressed air. The UHMWPE disks were scrubbed with a nonabrasive detergent, rinsed with distilled water, and also dried with compressed air.

Experimental

The specimens were inserted into the apparatus and the chamber was sealed. Moist air (approx. 50 percent RH) was purged through the chamber of 2000 cm^3 at the rate of 1500 cm^3/min for 15 minutes before commencing the test. The disk was set into rotation at the desired speed and a 9.8-N load was gradually applied. The test temperature was 24°±3° C (ambient).

Each test was stopped either after 20 or 1000 cycles of sliding. The pin and disk were removed from the apparatus and the contact areas were examined by optical microscopy and photographed. Surface profiles of the disk wear track were also taken. The specimens were then placed back into the apparatus and the test procedure was repeated. The pin was not removed from the holder, and locating pins ensured that it was returned to its original position. Each test was stopped and this procedure repeated at various sliding intervals up to 10 000 kilocycles.

The experimental method used to determine the effect of speed on friction was to first "run-in" the specimens at 1 rpm for 20 min. Then a series of 5

minute tests were performed at each of the following speeds: 0.25, 1, 10, 50, 100, 400, and 800 rpm. The speed was first increased from 1 to 800 rpm, then decreased to 0.25 rpm, and finally increased again to 800 rpm. Thus, for most of the speeds, three tests were made.

Surface Analysis

Visible light optical microscopy was used to study the wear surfaces, the transfer films, and the wear particles in this investigation. The surfaces were viewed with good resolution to magnifications of 2000. At these high magnifications, the depth of focus was very small (1 μm); this feature was used in measuring the heights of various features on the sliding surfaces, such as transfer film thickness and wear track depth.

The microscope was also equipped with two polarizing filters (one that could be rotated); thus the sliding surfaces could be examined between crossed polarizing filters. Birefringent particles observed by this method indicated that the particles had an anisotropic crystalline structure.

RESULTS AND DISCUSSION

Friction Coefficients

Average friction coefficients are plotted in Fig. 2 as a function of sliding duration in cycles (1 cycle equals 0.13 to 0.19 m) for the sliding speeds of 1, 10, 100, and 800 rpm. In general, the initial friction coefficient for any individual experiment was lower than its average value for the duration of the experiment. For sliding speeds of 10, 100, and 800 rpm, it took about 1000 cycles of sliding before the friction coefficient stabilized at 0.13±0.03 (± factor is due to variation from test to test and to sliding duration). The friction coefficient for the experiment conducted at 1 rpm remained constant at 0.05±0.02 for the duration of the experiment (4300 cycles).

To investigate further the effect of sliding speed on the friction coefficient, an experiment was devised whereby the friction coefficient was measured at sliding speeds of 0.25 to 800 rpm all on the same wear track (see the section Procedure). Figure 3 gives those results, which indicate that both sliding duration and sliding speed affect the friction coefficient. In general, the friction coefficient increased as speed was increased, although at speeds below 10 rpm the effect was minimal.

UHMWPE Wear

UHMWPE wear was studied by taking surface profiles of the disk wear track after each sliding interval. Figure 4 give representative surface profiles for the 10-, 100-, and 800-rpm sliding speed tests after various sliding durations. Because the vertical magnification of the surface is about 40 times the horizontal magnification, the view of the surface is distorted.

The surface profiles show that the wear process was one of gradual wear through the UHMWPE disk. The profiles also indicate that plastic deformation has occurred at the sides of the wear track. Another interesting phenomenon is that the wear track surfaces on the UHMWPE disk for the 10- and 100-rpm tests (also the 1 rpm test, which is not shown) were very rough; but the tests at 800 rpm produced surfaces that were very smooth (Fig. 4). Possible reasons for this are discussed in the section UHMWPE Wear Surface Morphology.

To quantify the wear process, wear volume was calculated by measuring the cross-sectional area of the wear tracks (from the surface profiles) after each sliding interval and multiplying it by the circumference of the tracks. At least four different traces at different positions were taken at each interval. Wear rate in terms of wear volume (in m^3) per unit sliding distance (in m) was calculated for each sliding interval. These incremental wear rates are listed in Table 1 and plotted in Fig. 5 as a function of sliding dis-

tance. Wear rate for the first 10 meters of sliding was very high, of the order of 10^{-11} m^3/m of sliding. As sliding distance increased, the rate decreased until about 10 000 meters; after this point the rate tended to level off. Even after it leveled off, there was still quite a variation in the wear rate from $4x10^{-14}$ to $4x10^{-15}$ m^3/m of sliding. Sliding speed had no apparent effect on wear rate.

Since the wear rate in the initial stages of sliding was very high and since the average contact stresses with this geometry generally decrease as wear occurs, it was postulated that decreasing average contact pressure may have been responsible for the decreasing wear rates which occurred with increasing sliding duration. Figure 6 plots incremental wear rate as a function of average contact pressure for each test. Average contact pressure was determined by dividing the load by the projected contact area. The projected contact area was approximated by measuring the transfer film (or contact area on the pin) and the surface profiles on the UHMWPE disk wear track. Figure 6 shows that the incremental wear rate decreases exponentially with decreasing contact stress.

Rider Transfer Morphology

Polymer transfer to the metallic pin was studied with a light microscope during the intervals when the tests were stopped. Interval observation of the surfaces during the initial stages of sliding showed individual platelets of UHMWPE and striations in the sliding direction which indicated the platelets were flowing through the contact area. Also on subsequent observation at the next interval, the platelets were never in the same place. UHMWPE also tended to fill in the small scratches on the metallic pin surface.

On observing the surfaces for longer sliding intervals, it was seen that the transfer tended to increase with sliding duration. But the amount and

type tended to depend on the sliding speed. At speeds of 1-, 10-, and 100-rpm very heavy ridges of transfer built-up; but a 800-rpm, only thin, flowing transfer films (less than 1 μm) occurred.

Examples of the different types of transfer are shown in Figs. 7 to 9. In Fig. 7, transfer to the pin is shown after 3200 cycles of sliding at 1 rpm. A considerable buildup of transfer is evident in the rider contact entrance region. Emanating from this material are fibrous crystalline structures. The origin of these structures is not certain, but they appear to be produced on the UHMWPE disk wear track, from which they eventually disengage, and then are collected in the rider entrance. Some are forced into the contact area, where they become attached and give the appearance that they are being produced from the rider transfer.

In addition to the fibrous structures, there are ridges of heavy transfer on the pin, and plastically deformed UHMWPE material in the exit region (see blowup in Fig. 7). The UHMWPE material appears to have flowed across the pin contact area and coalesced to form the structure shown in Fig. 7.

The transfer films formed at 10 rpm were very similar to those formed at 1 rpm. The transfer films formed at 100 rpm looked slightly different than those at 1 rpm, although some fibrous structures were seen. Figure 8(a) shows a typical transfer film for this sliding speed. Heavy ridges of UHMWPE transfer material have built-up on the pin contact area.

At 800 rpm, the transfer was very different from the slower speed tests. Figure 8(b) shows typical transfer to a pin that slid at 800 rpm. No ridges of UHMWPE transfer occurred, instead very thin transfer (less than 1 μm) was observed in which interference fringes could be seen. The transfer remained thin for the duration of the tests. Figure 9 presents two other interesting features in transfer morphology that were observed at 800 rpm. In the inlet

area of the pin, "fiber-like" bundles of birefringent UHMWPE were observed (Fig. 9(a)). And in the pin exit region, birefringent "icicle-like" structures were observed (Fig. 9(b)). Especially the "icicle-like" structures suggest that some degree of melting has taken place. Optical pyrometer temperature measurements of the pin tip (not the contact area) indicate that the temperature at 800 rpm exceeds 70° C; while at 100 rpm, temperatures of only 32° C were recorded.

UHMWPE Wear Surface Morphology

For short sliding distances the wear surface morphology did not seem to depend on sliding speed. Some of the wear features observed on the wear tracks are shown in Fig. 10. Figure 10(a) shows raised "roll type" of wear particles, Fig. 10(b) shows wear grooves and "back-transfer" wear particles, and Fig. 10(c) shows a "glassy-looking" wear particle with iridescent speckles in it. Figures 10(c) and (d) also show very thin, plastically flowing surface layers.

For long sliding distances, the wear surface morphology for the 800-rpm experiments did not change; but for the slower speed experiments, a new wear feature emerged. Figure 11 compares the UHMWPE wear surfaces for the 100- and 800-rpm experiments after 400 kc (65 km) and 1500 kc (245 km), respectively. Figure 11(a) shows a photomicrograph of the 100-rpm experiment which was taken between crossed polarizing filters. Birefringent bands can be seen in the wear track running parallel to the rider sliding direction and birefringent wear debris is seen extending outward from the edge of the wear track. These birefringent bands were not observed at the 800-rpm sliding speed (Fig. 10(b)).

It is believed that the birefringent bands observed at 100-rpm and at slower speeds are caused by the buildup of heavy ridges of transfer (Fig. 8(a)). This type of transfer induced localized high stresses on the UHMWPE

disk wear track, and repeated passes of the surface induced orientation and an anisotropic crystalline material. Eventually the crystalline material disengaged from the surface, leaving a groove, and accumulated at the side of the wear track (Fig. 11(a)) or in the rider inlet area (Fig. 7). Because grooves were left behind on the wear track, the surfaces were rougher at the slower sliding speeds (Fig. 4).

An additional type of wear particle observed at the 800-rpm sliding speed was a birefringent cylindrical wear particle. This type was found in the exit area of the pin (Fig. 12(b)) or outside of the pin wear track. The author has also observed this type of wear particle with polyimides (Ref. 10). They were postulated to be caused by thin transfer films rolling up as they leave the exit region of the contact area or by thin polymer surface layers rolling up and disengaging from the surface. Birefringent spherical wear particles (Fig. 12(b)) were also observed at 100- and 800-rpm. Generally, these were found outside the wear track area. No speculation is given on their formation.

Another wear phenomenon was observed in one experiment at 800-rpm. The UHMWPE disk either had a hard-particle inclusion, or a hard particle was deposited on the wear track during one of the intervals in which the specimens were being examined. Figure 13 shows the wear caused by this hard particle. A deep groove was worn on the metallic rider (Fig. 13(a)) by the particle (Fig. 13(b)); and subsequently a circumferential ridge occurred on the UHMWPE disk (Fig. 13(c)) due to the rider groove. The figure points out that third-body wear caused by foreign contaminants can be very detrimental to sliding constituents. This is especially true of polymers, which are very susceptible to hard particles embedding in them.

REMARKS

This study indicates that the plastic deformation of thin surface layers is a necessary factor in providing self-lubrication; however, if contact stresses (pressures) become too high, gross deformation and premature failure can occur. The problem is to control contact stresses so that only the deformation of thin surface layers occurs.

Plastic deformation of the surface layers produces ordered wear particles, when they find their way out of the contact zone. Birefringent platelets, ribbons, cylinders and spheres were observed. But when the particles remain within the contact zone, they are back-transferred back and forth between the sliding surfaces. Less order occurs and the particles are not completely birefringent. The particles tend to flatten-out and attach themselves to the UHMWPE wear surface. They also tend to flow very slowly on the surface and produce very small "roll-type" wear particles.

UHMWPE has the ability to "plastically flow into itself." That is, either a surface layer or a wear particle has the ability to plastically flow into another wear particle or surface layer and to produce a new continuous entity which has no lines of demarcation. This phenomenon of "flowing into itself" seems to be a prerequisite of all good self-lubricating solid lubricant materials.

COMPARISON WITH OTHER WORK

Jones, et al. (Ref. 9) have conducted similar experiments on the identical UHMWPE material (RCH 1000). Their experiments were conducted using the same apparatus, but differed in that hemispherically tipped UHMWPE riders were slid against AISI 316L stainless steel disks with a surface roughness of 0.038 μm cla. They found that the friction coefficient initially increased from 0.28 to 0.55 with sliding distance for the first 2 to 3 km of sliding.

It then gradually declined during the next 17 km of sliding and eventually stabilized at 0.44±0.07. The calculated wear rate from their experiments was $(1.6\pm0.7)\times10^{-15}$ m^3/Nm. In this study, friction coefficient also tended to increase with sliding duration but stabilized at 0.13±0.03 after about 300 meters of sliding. The wear rate in their units was $(2.2\pm1.8)\times10^{-15}$ m^3/Nm.

Fairly good correlation of wear rates between the two configurations was obtained, but friction coefficients were completely different (0.13 vs. 0.44). A possible reason for the difference is that the Jones, et al., experiments used a different stainless steel with a smoother surface finish (316L, 0.038 μm cla). Also, and probably most important, Jones' experiments were conducted in dry air (<50 ppm H_2O) instead of in moist air (10 000 ppm H_2O). Another possible reason for the difference may have been the geometry differences. A similar phenomenon occurred when graphite-fiber-reinforced polyimide (GFRPI) composites were evaluated in these two geometries (Ref. 11). The friction coefficient for the GFRPI pin sliding on the metal disk at 25° C was 0.24; the opposite combination was 0.19. As temperature increased, the differences became more pronounced, and at 300° C the friction coefficient for the GFRPI pin sliding against the disk was 0.76, while for the opposite combination it was 0.05.

Atkinson, et al. (Ref. 8) have also evaluated the same type of UHMWPE (RCH 1000) in a three-pin-on-disk tribometer. They reported a lower wear rate of $(2.4\pm1.8)\times10^{-16}$ m^3/Nm, about 10 times less wear. A possible reason for this is that three truncated UHMWPE cones rather than a hemisphere were used, and thus lower initial contact stresses were obtained. Three pins would also affect transfer film characteristics. An unknown quantity in their tests is the atmosphere: the tests were run in air, but the humidity was not given. In Atkinson's et al., experiments sliding speed was 0.24 m/s, and applied

forces of 25.0 to 155.5 N were evaluated as well as EN 58 J stainless steel counterfaces of 0.015 to 0.120 μm Ra.

Jones, et al. (Ref. 9) did not report any microscopic observations of the UHMWPE sliding surfaces; but Atkinson, et al. (Ref. 8) did. Many of the wear features reported by Atkinson, et al., were also observed in this study - such as "roll type" of wear particles (crescents), back-transfer particles, wear grooves parallel to the sliding direction, and ductile plastic flow.

One type of wear feature not observed by Atkinson, et al., was a "fatigue like" wear particle on the UHMWPE disk wear track that was postulated to be caused by repeated passes over the disk by the ridges of very heavy transfer. This process tended to cause the UHMWPE to crystallize into long, birefringent wear streamers or ribbons.

CONCLUSIONS

Tribological studies at 25° C in a 50-percent-relative-humidity air atmosphere with hemispherically tipped 440C high-temperature stainless-steel pins sliding against ultra-high-molecular-weight polyethylene (UHMWPE) disks led to the following conclusions:

1. Friction Coefficient...
   (a) Was lowest when contact area was smallest.
   (b) Increased with sliding speed.
   (c) Increased as thick transfer films were produced.
   (d) Was dependent on specimen contact configuration.
2. UHMWPE wear rate...
   (a) Was not dependent on sliding speed.
   (b) Was highly dependent on average contact pressure.

3. UHMWPE transfer to the pin...

   (a) Increased with sliding distance for sliding speeds of 1, 10, and 100 rpm, resulting in the buildup of thick ridges of UHMWPE material.

   (b) Was thin and plastically flowing at 800 rpm and did not build up with sliding distance.

4. Wear Mechanism...

   (a) Was adhesion at 800 rpm and for short sliding distances at 1, 10, and 100 rpm.

   (b) Was fatigue-like for long sliding distances at 1, 10, and 100 rpm, produced by the build up of UHMWPE transfer ridges on the pin.

   (c) Was plastic deformation, for high initial contact stresses.

   (d) Was abrasive when hard particles embedded in the UHMWPE disk and abraded the metallic pin.

REFERENCES

1. Manson, S. S., "New Directions in Materials Research Dictated by Stringent Future Requirements," National Aeronautics and Space Administration TM X-67885 (1971).

2. Sliney, H. E., and Jacobson, T. P., "Dynamic Load Capacities of Graphite-Fiber: Polyimide Composites in Oscillating Plain Bearings to 340° C (650° F)," National Aeronautics and Space Administration TN-7880 (1975).

3. Bangs, S., "Foil Bearings Help Air Passengers Keep Their Cool," Power Transm. Des., 15 (2), 27-31 (1973).

4. Blok, H., and van Rossum, J. J., "The Foil Bearing - A New Departure in Hydrodynamic Lubrication," Lubr. Eng., 9 (6), 316-320 (1953).

5. Ma, J. T. S., "An Investigation of Self-Acting Foil Bearings," J. Basic Eng., 87 (4), 837-846 (1965).

6. Sonstegard, D. A., Matthews, L. S., and Kaufer, H., "The Surgical Replacement of the Human Knee Joint," Sci. Am., 238 (1), 44-51 (1978).

7. Walker, P. S., and Erkman, M. J., "The Wear of High Molecular Weight Polyethylene with Particular Reference to its Use in Human Joints," Advances in Polymer Friction and Wear, ed. by L. H. Lee, Plenum (1974), pp. 533-511.

8. Atkinson, J. R., Brown, K. J., and Dowson, D., "The Wear of High Molecular Weight Polyethylene," J. Lubr. Technol., 100, 208-218 (1978).

9. Jones, W. R., Jr., Hady, W. F., and Crugnola, A., "Effect of Irradiation on the Friction and Wear of Ultrahigh Molecular Weight Polyethylene," Wear, 70, 77-92 (1981).

10. Fusaro, R. L., "Tribological Properties and Thermal Stability of Various Types of Polyimide Films," ASLE Trans., 25 (4), 465-477 (1982).

11. Fusaro, R. L., "Geometrical Aspects of the Tribological Properties of Graphite-Fiber-Reinforced Polyimide Composites," National Aeronautics and Space Administration TM-82757 (1982).

TABLE 1. - UHMWPE WEAR RATES FOR SELECTED SLIDING INTERVALS AND SLIDING SPEEDS

Sliding interval, kilocycles	Experiment number										
	1	2	3	4	5	6	7	8	9	10	11
	Sliding speed, rpm										
	1	10	100				800				
	Incremental wear rate, m^3/m										
0 - 0.02	450×10^{-13}	220×10^{-13}	---	---	60×10^{-13}	---	---	---	---	---	---
0 - 1.0	---	---	---	---	---	21×10^{-13}	---	60×10^{-13}	8×10^{-13}	20×10^{-13}	24×10^{-13}
.02 - 1.0	11	15	---	---	11	---	---	---	---	---	---
1 - 10	3	.5	---	---	2	2	---	2	3	3	2
10 - 20	---	.3	0.2×10^{-13}	---	1	---	---	.4	.5	2	1
20 - 60	---	.2	.1	0.3×10^{-13}	.2	.2	0.5×10^{-13}	.3	.1	.8	.7
60 - 100	---	.2	.2	.3	.06	.1	.4	.2	.1	.2	.4
100 - 200	---	.2	.04	.3	.1	.1	.06	.02	.1	.2	.3
200 - 400	---	---	.3	.1	.1	.1	.1	.06	.1	.09	.2
400 - 600	---	---	.4	.4	.1	.1	.1	.06	.2	.04	.1
600 - 1000	---	---	.3	.05	.1	.2	.1	.03	.06	.04	.1
1000 - 1500	---	---	---	---	.04	.1	---	.06	.1	.04	.1
1500 - 2000	---	---	---	---	.07	.1	---	.05	.2	.04	.07
2000 - 3000	---	---	---	---	.08	.1	---	.06	.2	.06	.07
3000 - 4000	---	---	---	---	.06	.1	---	.06	---	.09	---
4000 - 5000	---	---	---	---	---	.2	---	---	---	.04	---
5000 - 7500	---	---	---	---	---	.04	---	---	---	.04	---
7500 - 10000	---	---	---	---	---	.04	---	---	---	.04	---

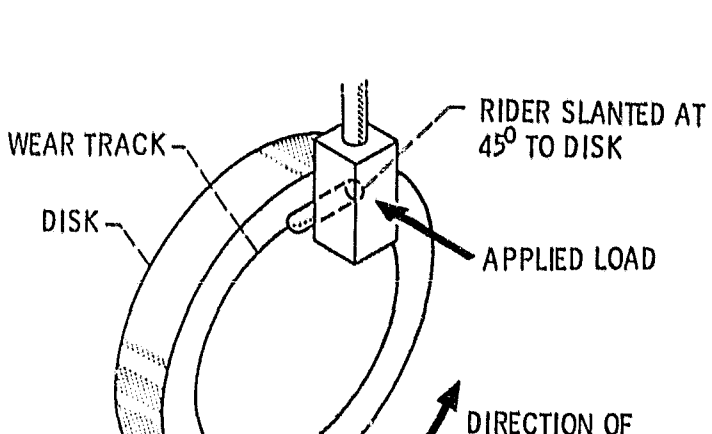

Figure 1. - Schematic diagram of friction specimens.

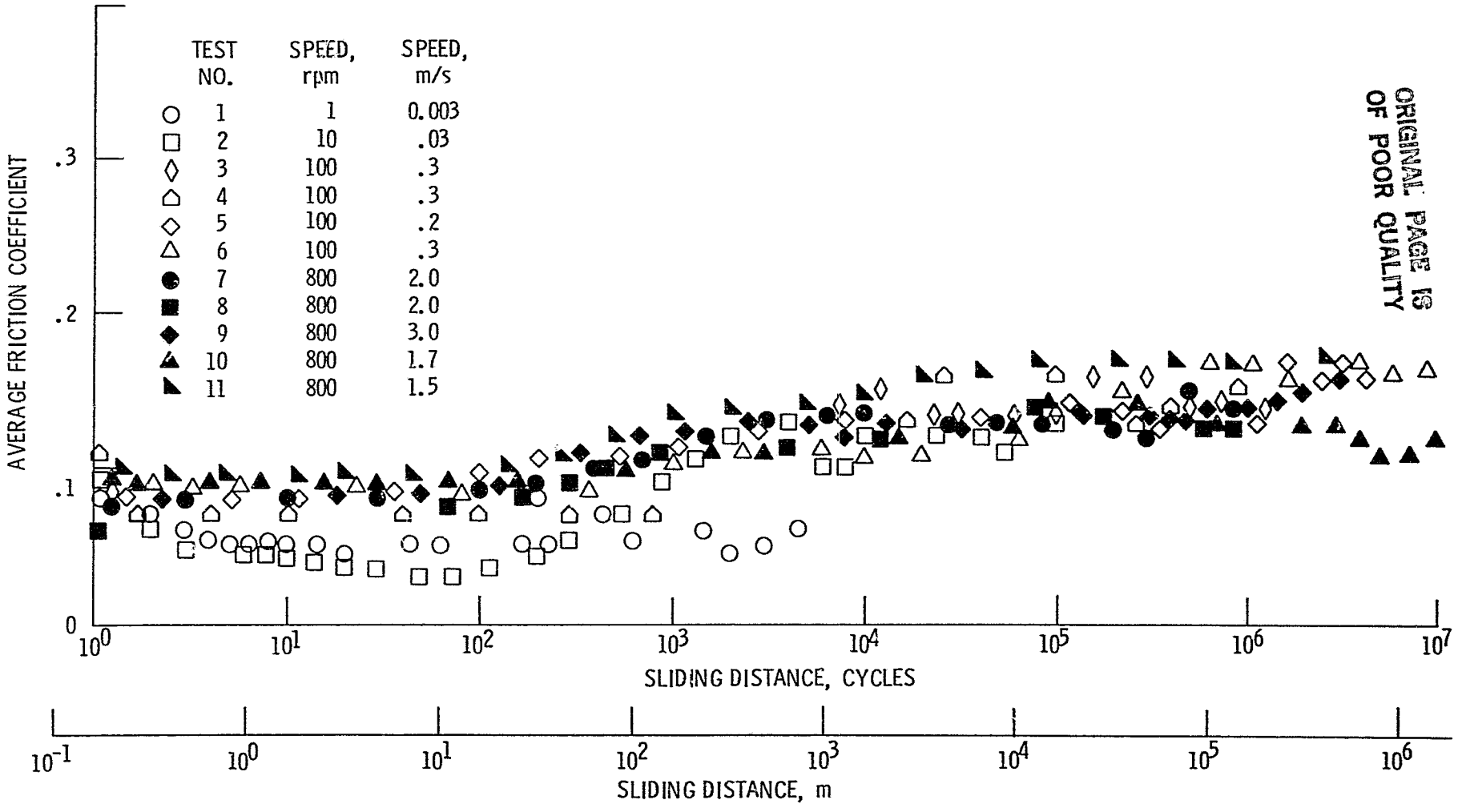

Figure 2. - Average friction coefficient as a function of sliding distance for a hemispherically tipped 440C HT stainless steel pin sliding against a UHMWPE disk at various sliding speeds at ambient temperature (25^0 C) under a 9.8 N load in a 50% relative humidity atmosphere.

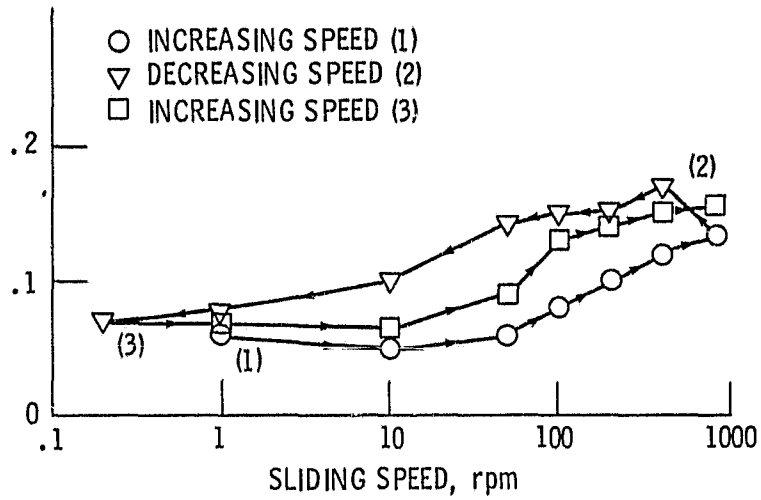

Figure 3. - Average friction coefficient as a function of sliding speed for a hemispherically tipped 440C HT stainless steel pin sliding against a UHMWPE disk at ambient temperature (25° C) under a 9.8 N load in a 50% relative humidity air atmosphere. Sliding time at each speed was 5 minutes.

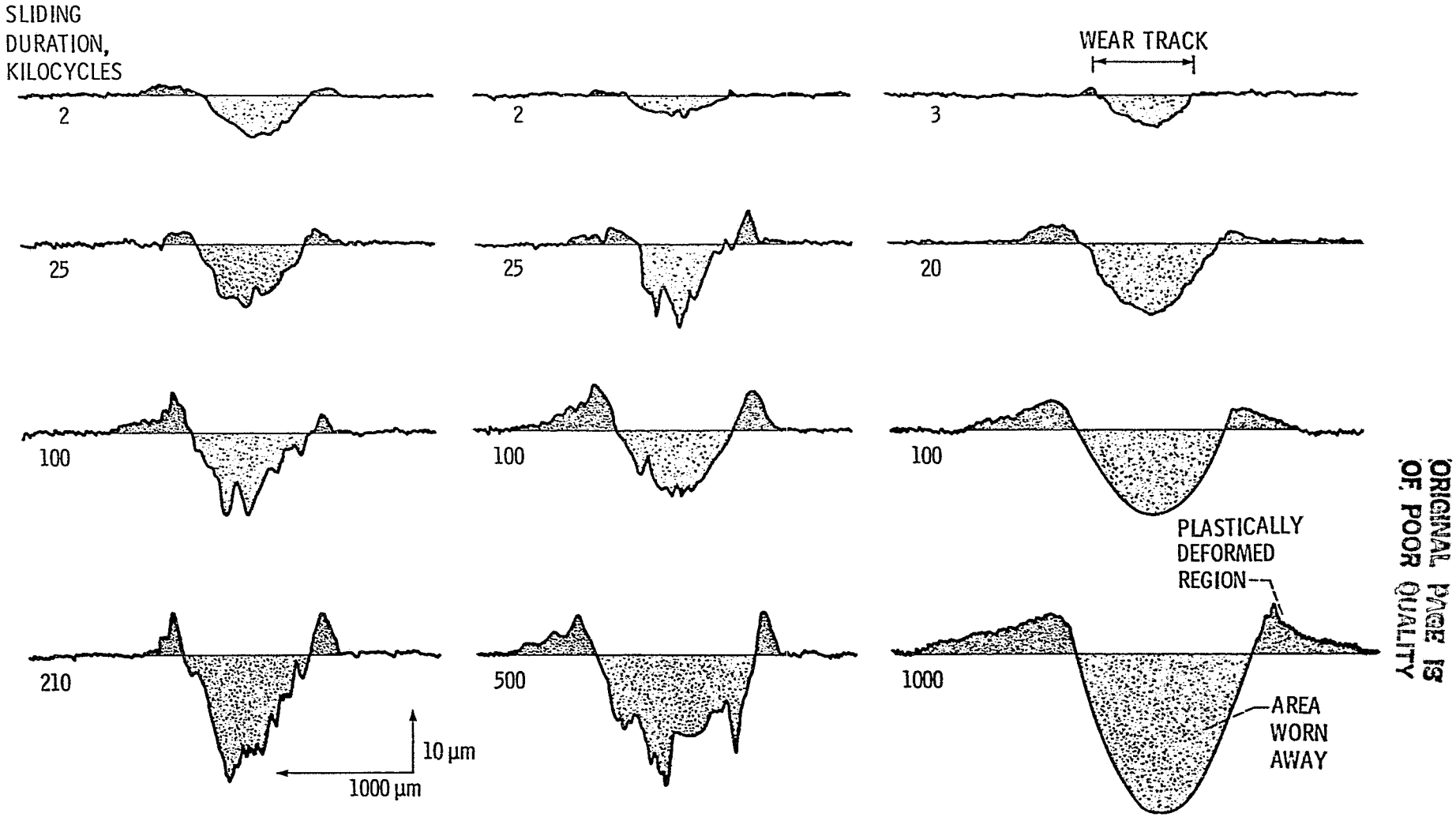

(a) Sliding speed, 10 rpm.

(b) Sliding speed, 100 rpm.

(c) Sliding speed, 800 rpm.

Figure 4. - Surface profiles of wear tracks on UHMWPE disks after various sliding distances and speeds.

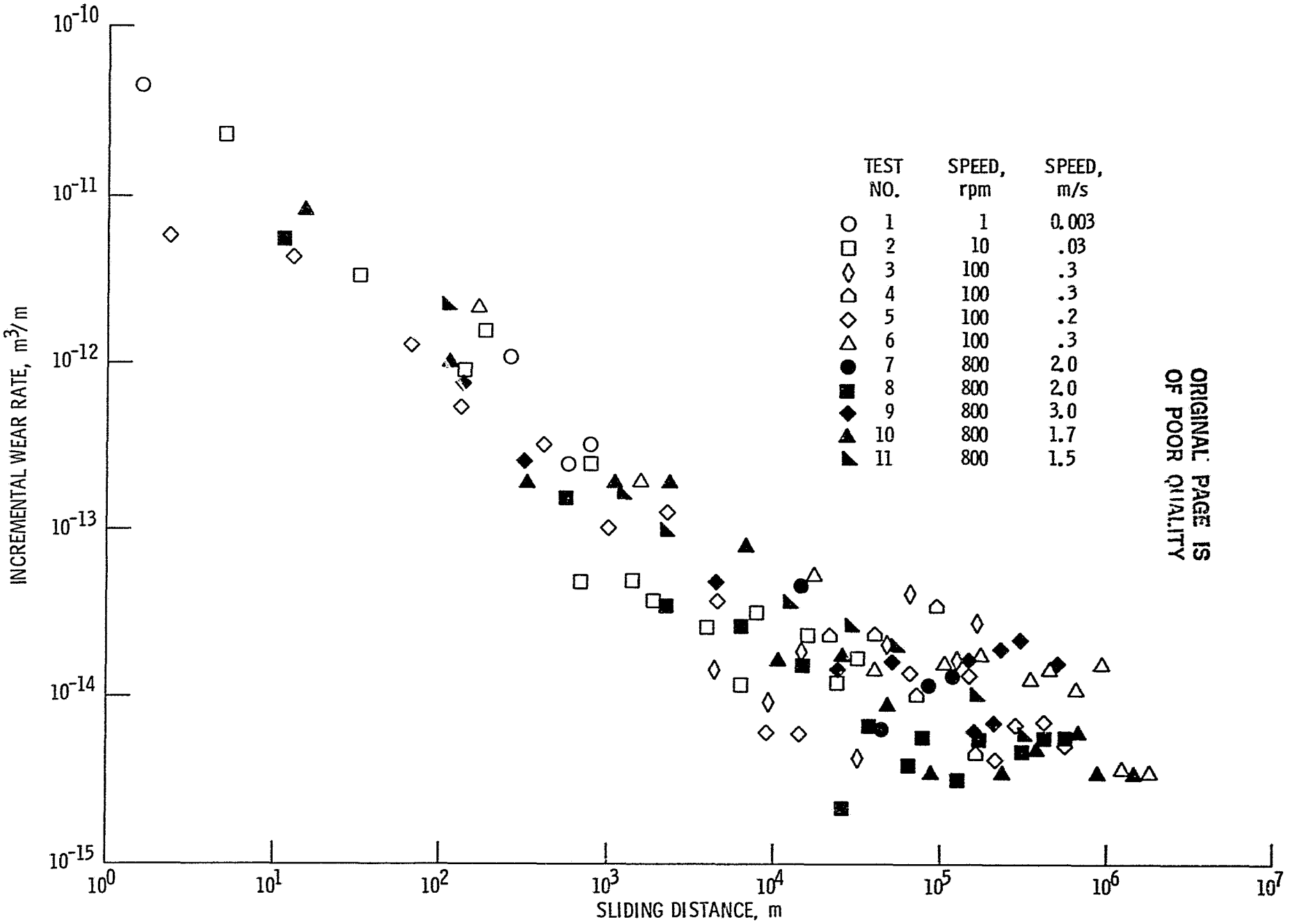

Figure 5. - UHMWPE Incremental Wear Rate as a function of sliding distance for various sliding speeds.

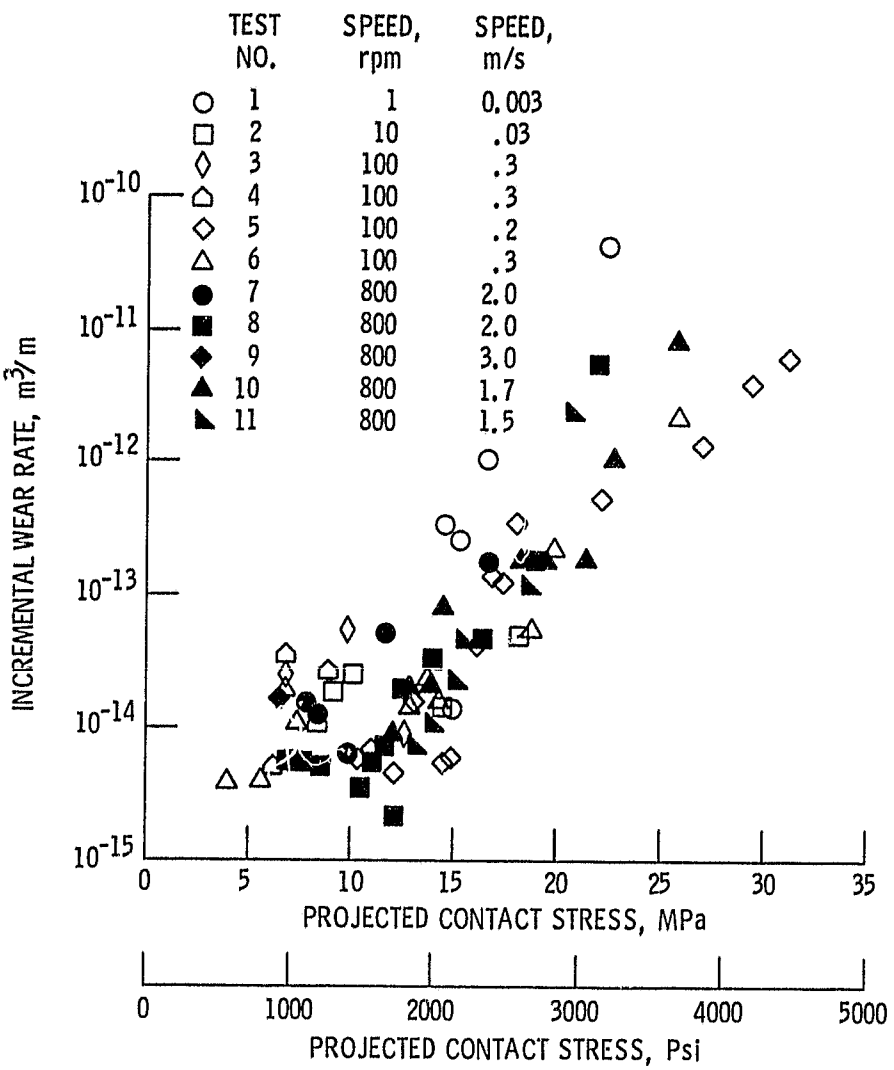

Figure 6. - UHMWPE incremental wear rate as a function of projected contact stress for various sliding speeds.

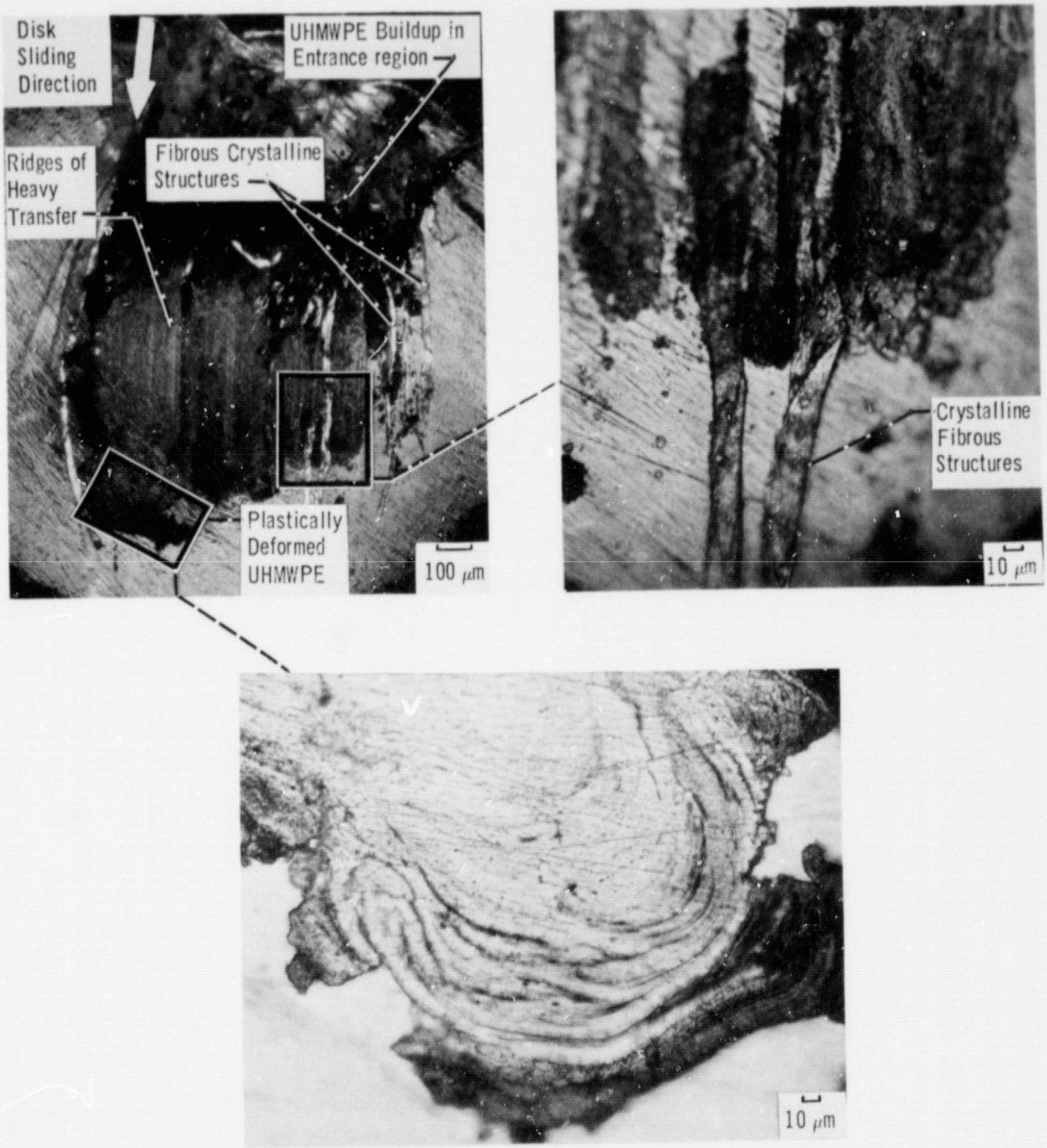

Figure 7. - Rider transfer film after 3.2 kc of sliding for a pin which slid on an UHMWPE disk at 1 rpm.

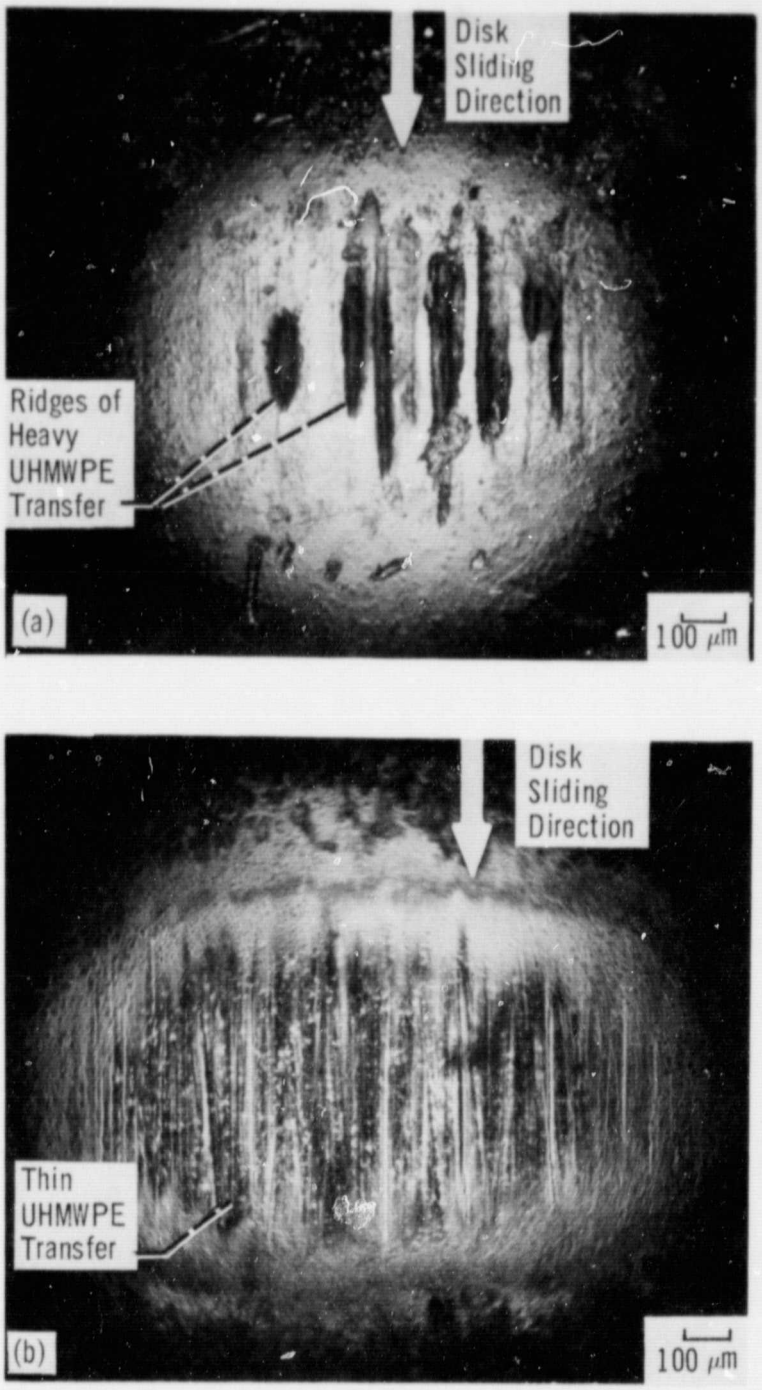

(a) 100 kc of sliding at 100 rpm.

(b) 3000 kc of sliding at 800 rpm.

Figure 8. - Transfer to a pin sliding on UHMWPE at (a) 100 rpm and at (b) 800 rpm.

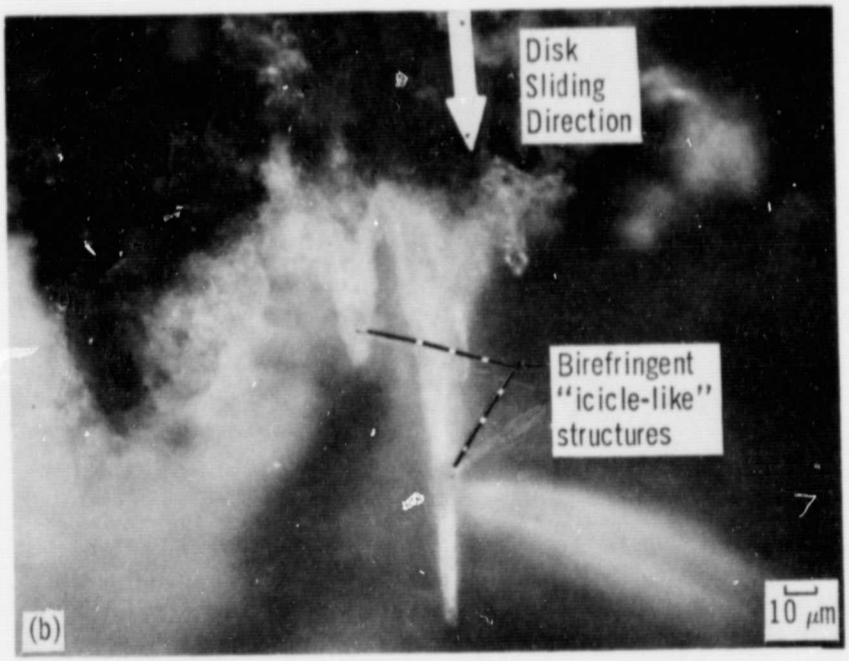

(a) Pin inlet area.

(b) Pin exit area.

Figure 9. - Birefringent "fiber-like" bundles and "icicle-like" structures found in the pin inlet areas and pin exit areas, respectively, for experiments conducted at 800 rpm (1.7 m/s).

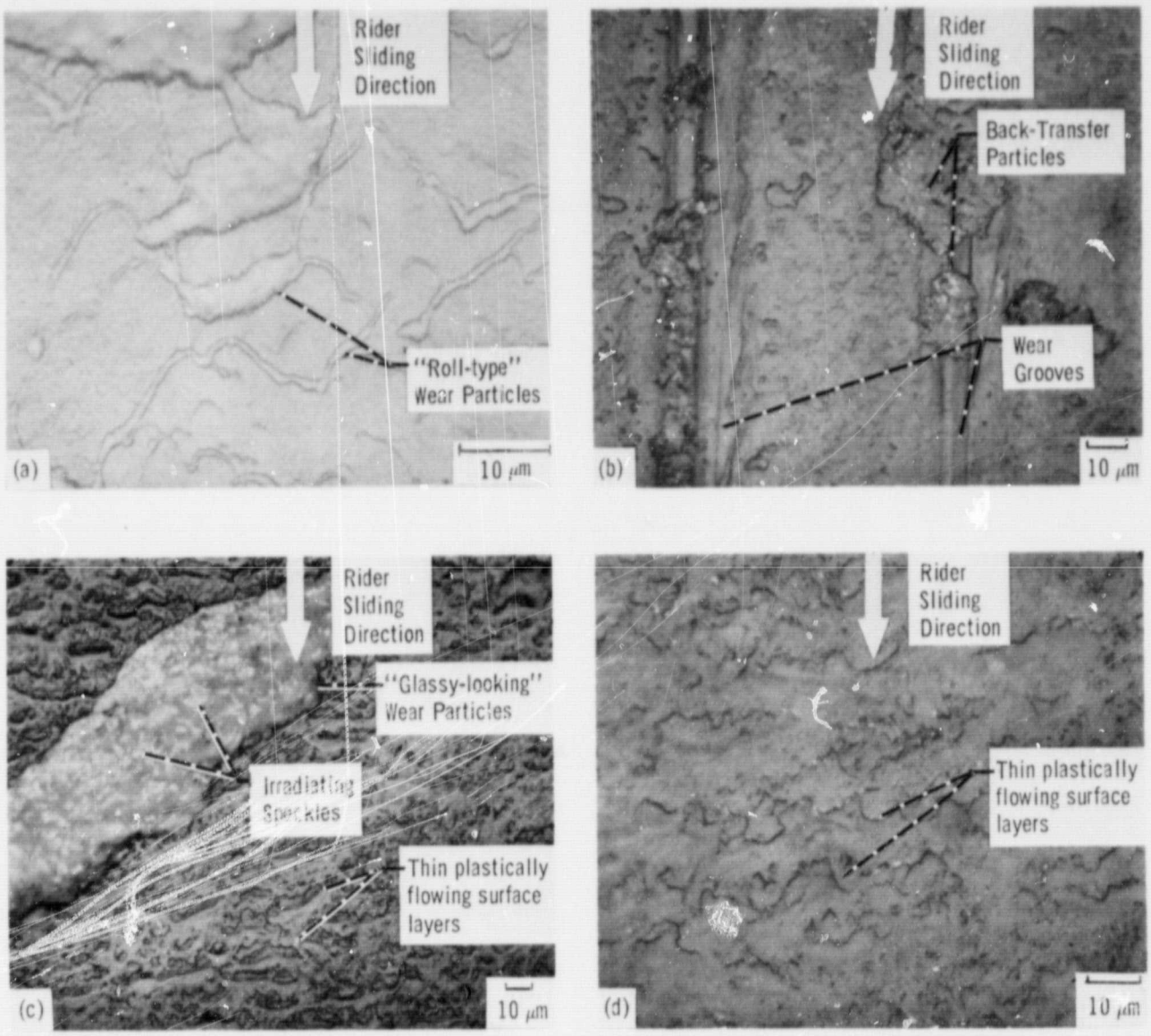

(a) Raised "roll-type" wear particles.

(b) Wear grooves and back transfer.

(c) "Glassy-looking" wear particles.

(d) Plastically flowing surface layers.

Figure 10. - Representative photomicrographs showing the various wear features observed on the UHMWPE wear tracks.

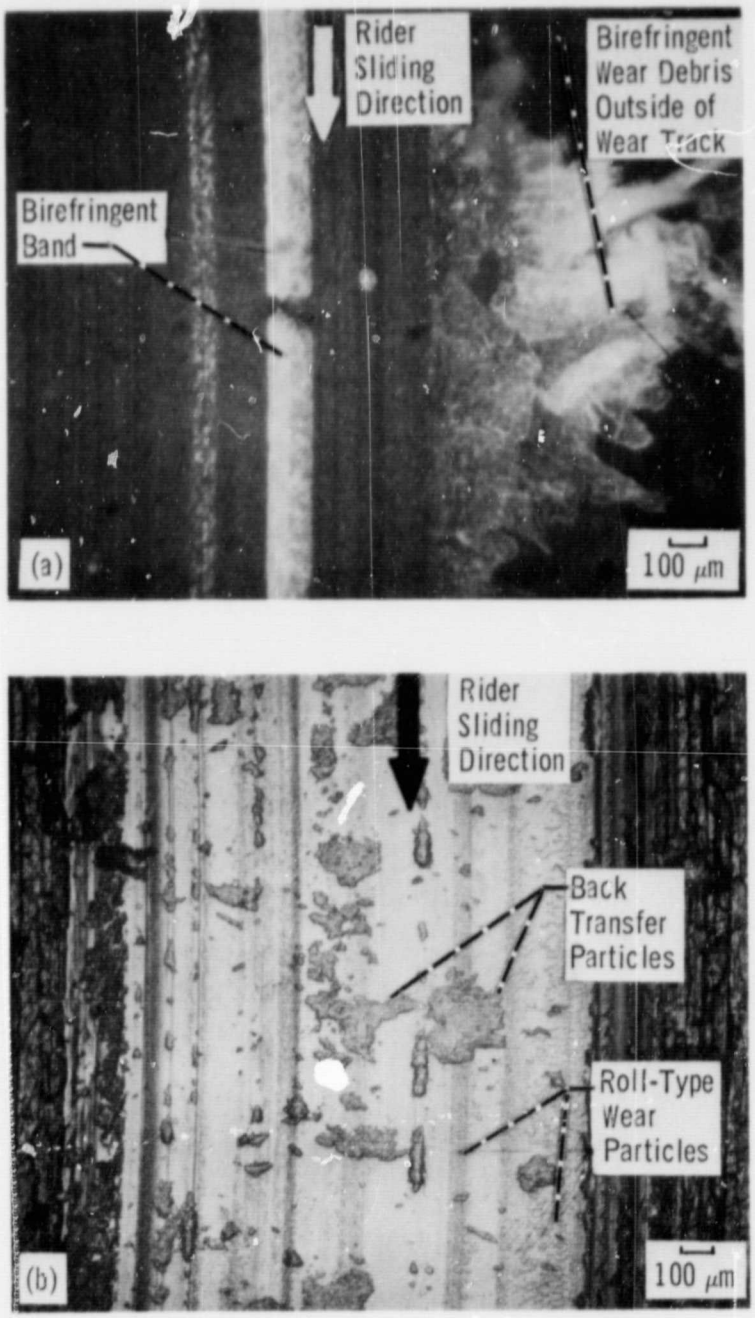

(a) 400 kc of sliding at 100 rpm. (Photograph taken with specimen between crossed polars.)

(b) 1500 kc of sliding at 800 rpm.

Figure 11. - Photomicrographs of the wear tracks on UHMWPE disks after (a) 400 kc of sliding at 100 rpm and (b) 1500 kc of sliding at 800.

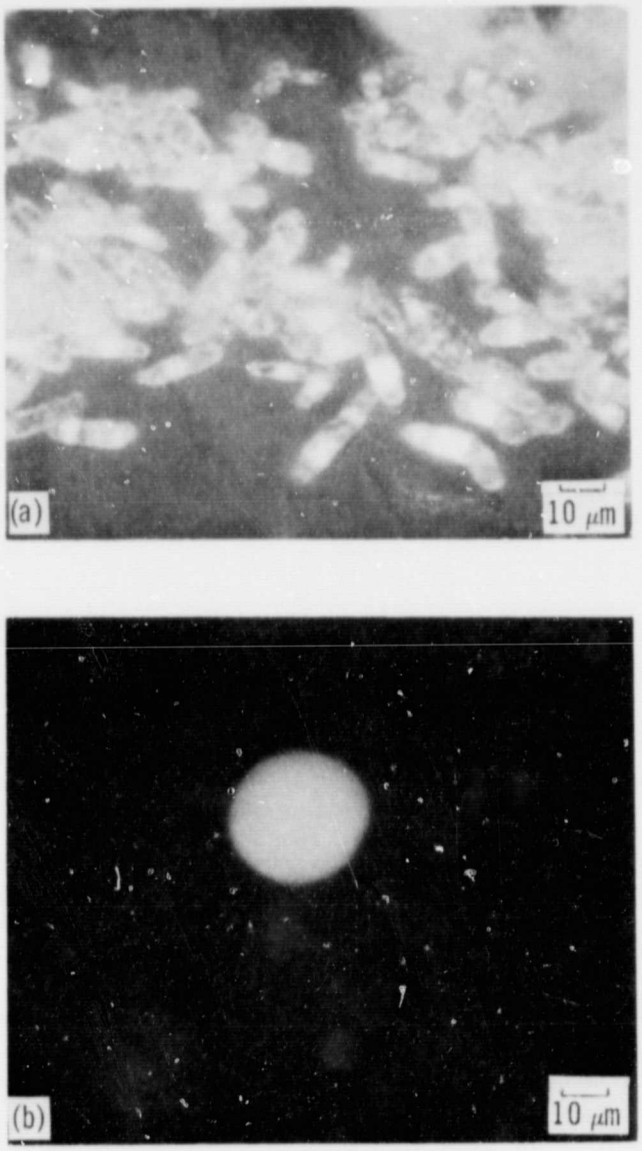

(a) Cyclindrical wear particles.

(b) Birefringent spherical wear particle.

Figure 12. - Birefringent cylindrical wear particles found in pin exit area and birefringent spherical wear particle found outside of UHMWPE disk wear track.

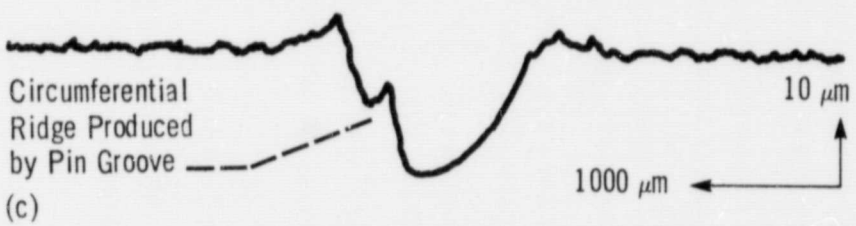

(a) Photomicrograph of metallic pin contact area.

(b) Photomicrograph of UHMWPE disk wear track.

(c) Surface profile of UHMWPE disk wear track.

Figure 13. - Photomicrographs and a surface profile of the sliding contact areas illustrating the wear caused by an embedded hard particle in the UHMWPE disk.